On model simplification of launch vehicle rigid body dynamics

Adolfo G. Silva, Waldemar C. Leite Filho** and Alexandro G. Brito***
**Instituto Nacional de Pesquisas Espaciais*
Av. dos Astronautas, 1758, Jd. da Granja. CEP: 12227-010 São José dos Campos-SP Brazil
***Instituto de Aeronáutica e Espaço*
Pça Mal. Eduardo Gomes 50, vila das Acácias. CEP: 12228-904 São José dos Campos-SP Brazil

Abstract
This paper discusses the launch vehicle dynamics and the assumptions to obtain the rigid body simplified equations. It is seen that a very simplified rigid body transfer function may be unsuitable to calculate the controller gains if a highly unstable rocket is considered. Moreover, a PD or PID controller cannot reach the time domain requirements with this type of vehicle configuration. Then, a more complete transfer function should be used and a PD plus phase-lag structure is proposed to accomplish these requirements and to achieve the stability margins.

1. Introduction

The design of the launch vehicle attitude control system represents a challenging flex-body problem since its nonlinear time-varying coupling equations. The main design objectives are good tracking and robust stability, and the controller synthesis used to be a hard multi-objective optimization problem [1]. Before applying any optimization algorithm, it is necessary to obtain the mathematical launch vehicle model [2], [3]. A common approach to design the attitude control system is to split the launch vehicle dynamics into the rigid and flex body dynamics, under the assumption that a negligible interaction between the two dynamics exists [2]. Moreover, to permit a linear analysis using the common control techniques (such as frequency responses diagrams, root locus and etc.) it is necessary to assume that the vehicle parameters do not change over a short period of time, even though it slowly changes. By using the linear analysis, it is possible to understand the vehicle features effects on the attitude control system. New design methods synthesize a robust controller and flex-filters, which aims the stability margins maximization while achieving the time domain requirements performance [4], [5]. These new methods are promising but they can lead to lack of problem insight by the designer.

This article treats the rigid body dynamics and its simplification to obtain a second order transfer function. If the vehicle is highly unstable, the second order transfer function cannot properly represent the vehicle dynamics. This issue is discussed herein. Furthermore it is shown that a PD or PID controllers may not offer an acceptable time domain response for this type of vehicle configuration. Thus, a PD plus phase-lag structure is proposed to overcome this problem. This controller is designed based on the insights given by the rigid body dynamics analysis.

2. Rigid Body Equations

Consider Figure 1, which shows the forces acting on the vehicle at pitch plane. The rigid body dynamics is obtained through the equilibrium of moments and forces acting on the vehicle. To permit a linear analysis some assumptions are made, such as the vehicle trajectory is following a zero lift path (gravity turn strategy). Then, at steady state, the pitch rate, $\dot{\theta}_0$, is adjusted to cancel the transverse forces (gravitational) on the vehicle. From this assumption, the system is analyzed around the reference trajectory by performing a linear perturbation of the variables. In this way, a set of linear equations is obtained and, finally, the transfer function from the actuator command to the control variable is obtained by assuming that the vehicle parameters are frozen over a short period time. This equation is given by [2]:

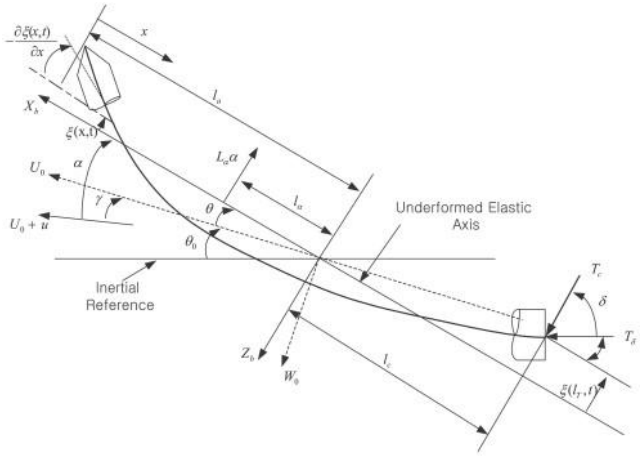

Figure 1- Launcher Vehicle Parameters [2]

$$G_c(s) = \frac{\theta(s)}{\delta(s)} = \frac{\mu_\delta s + \dfrac{Z_\alpha \mu_\delta + Z_\delta \mu_\alpha}{U_0}}{s^3 + \dfrac{Z_\alpha}{U_0} s^2 - \mu_\alpha s + \dfrac{\mu_\alpha g \cos\theta_0}{U_0}} = \frac{a_1 s + a_0}{s^3 + b_2 s^2 + b_1 s + b_0} \tag{1}$$

where, θ_0 is the nominal attitude angle, θ is the actual attitude, U_0 is the longitudinal velocity, μ_α is the aerodynamic moment (per unit of angle of attack), μ_δ is control moment coefficient (per unit of angle) and g is the gravitational acceleration. We also have

$$\mu_\alpha = \frac{L_\alpha l_\alpha}{I_y} \qquad Z_\alpha = \frac{L_\alpha}{m_T}$$

$$\mu_\delta = \frac{T_c l_c}{I_y} \qquad Z_\beta = \frac{T_c}{m_T}$$

where T_c is the control thrust, L_α is the normal aerodynamic force (per unit of angle of attack), l_c is the distance between the vehicle center of mass and the point where the control force is applied and l_α is the distance between the center of mass and center of pressure.

As well known in the literature [2], Eq. (1) can be simplified in two other equations, depending on the instant of flight and the vehicle characteristics. At the beginning of flight, the dynamic pressure is negligible, so Eq. (1) is simplified as

$$\frac{\theta(s)}{\delta(s)} = \frac{\mu_\delta}{s^2} \ . \tag{2}$$

When the forward velocity is high enough and the dynamic pressure is not negligible, Eq. (1) can be simplified as

$$G_s(s) = \frac{\theta(s)}{\delta(s)} = \frac{\mu_\delta}{s^2 - \mu_\alpha} \ . \tag{3}$$

This is the same to neglect the dipole next to the origin, which comes from the aerodynamic coupling between the translational and the rotational movement. Both, Eq. (2) and Eq. (3) properly represents the launch vehicle dynamics in most of the cases. However, there are some special cases whose Eq. (3) can lead to loss of information about the vehicle dynamics, as we will see hereafter.

Consider the launch vehicle parameters at maximum dynamic pressure given by the Table 1.

Table 1- Hypothetical launch vehicle parameters at maximum dynamic pressure

	μ_α (rad/s²)/rad	μ_δ (rad/s²)/rad	Z_α (m/s²)/rad	Z_δ (m/s²)/rad	g (m/s²)	U_0 (m/s)	Θ_0(°)
Values	4.3	7.0	50.8	19.2	9.8	595	18

The vehicle transfer function is given by

$$\frac{\theta(s)}{\delta(s)} = \frac{7\ s + 0.7388}{s^3 + 0.08571s^2 - 4.3s + 0.06736} = \frac{7(s+0.1055)}{(s^2 - 4.298)(s - 0.0157)} \tag{4}$$

Then, the simplified transfer function is

$$\frac{\theta(s)}{\delta(s)} = \frac{7}{s^2 - 4.3}\ . \tag{5}$$

The Bode diagrams of both Eq. (4) and Eq. (5) are shown in Figure 2. Note that, at the high frequencies ($f > \sqrt{\mu_\alpha}$), there is no difference between the simplified and non-simplified models. However, at the low frequencies, as the static gain as the phase characteristic are quite different. Therefore, it is expected that the simplified transfer function properly represents the transient behavior, but with a reasonable difference at the steady state.

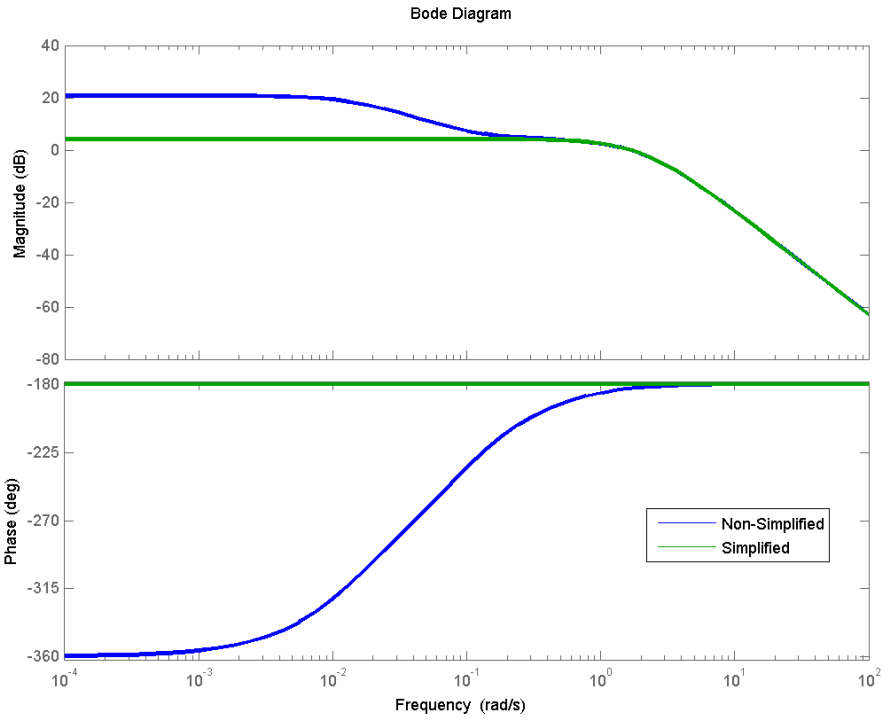

Figure 2 - Bode diagram of non-simplified and simplified rigid body dynamics

To emphasize this difference, PD and PID controllers will be designed to control the rigid body. In Figure 3, the simplified model of attitude control system is shown.

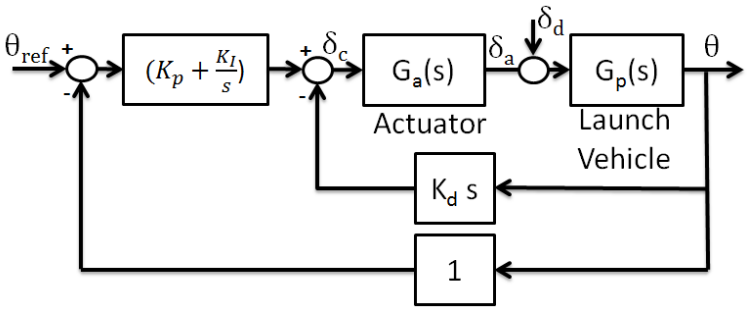

Figure 3 - Simplified attitude control system. It does not consider, for example, the bending mode

The actuator transfer function is assumed to be

$$G_a(s) = \frac{K_A}{s + K_A} \tag{6}$$

where K_A is the actuator bandwidth. Considering that the plant dynamics is given by Eq. (3), the closed loop transfer function with a PD controller is

$$G_{cl} = \frac{K_p K_A \mu_\beta}{s^3 + K_A s^2 + (K_A K_d \mu_\beta - \mu_\alpha)s + K_A(K_p \mu_\beta - \mu_\alpha)} , \tag{7}$$

and with a PID controller is

$$G_{cl} = \frac{K_A \mu_\beta (K_p s + K_I)}{s^4 + K_A s^3 + (K_d K_A \mu_\beta - \mu_\alpha)s^2 + K_A(K_p \mu_\beta - \mu_\alpha)s + K_A K_I \mu_\beta} . \tag{8}$$

Both controllers were designed to achieve some requirements, such as good stability margins, reasonable rise time and overshoot. Moreover, the gain crossover frequency is limited to enable further bending mode stabilization procedures. The PD design follows a pole placement based on choosing the natural frequency ω_n and damping ζ of the complex poles. Then, by considering the plant dynamics in Eq.(3), we have

$$D(s) = (s + p)(s^2 + 2\zeta\omega_n s + \omega_n^2) . \tag{9}$$

By comparing the coefficients of Eq. (9) with Eq. (7), the proportional and derivative gains can be calculated **.**

The PID gain computation follows the same methodology of the PD case: as the complex poles as the real pole p_I are specified. Then, the following characteristic equation is obtained

$$D(s) = (s + p)(s + p_I)(s^2 + 2\zeta\omega_n s + \omega_n^2) . \tag{10}$$

By comparing this equation with Eq. (8), the gains can be calculated .

Suppose that, the actuator bandwidth is K_A= 30 rad/s. The PD complex poles are specified so that ω_n=3.8 rad/s and ζ=0.9 to give the desired transient response. With this, the proportional and derivative gains are K_p=2.20 and K_d=0.84. The PID real pole is placed at p_I = -0.5 to improve the steady state error. Then, the PID gains are K_p=2.56, K_d=0.89 and K_I=0.78. By using these gains, the step response can be obtained as shown in Figure 4.

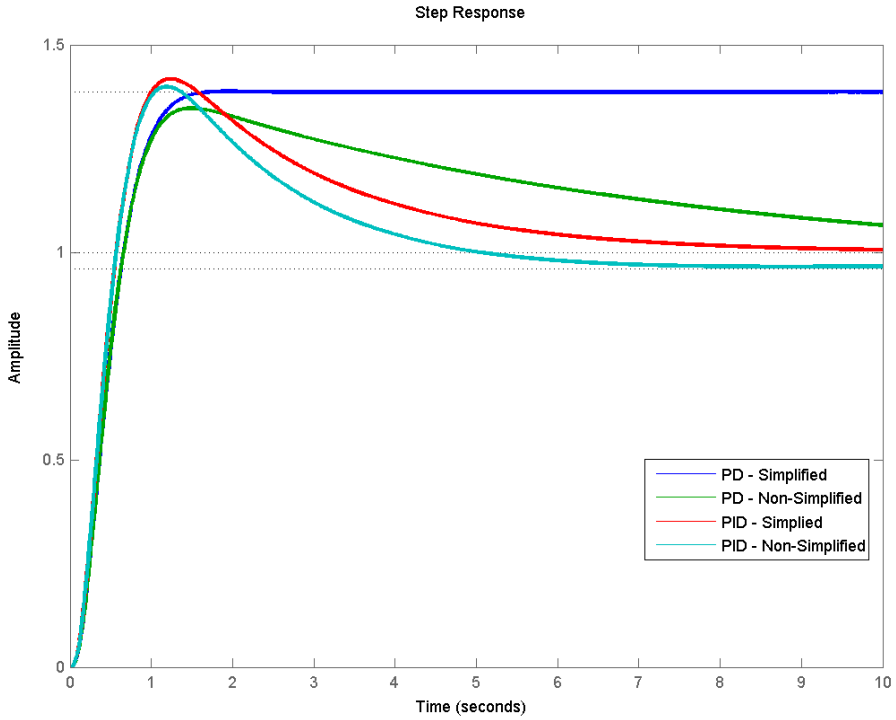

Figure 4-Step Response of PD and PID controllers

A physical interpretation of this step response, which corresponds to a typical highly unstable rocket, is possible: when a command is driven, the attitude begins to change and an angle of attack appears. Due to such angle, an aerodynamic moment is generated at the same direction of the control moment. In this way, a quick response and an overshoot are expected. However, when the actual orientation is higher than the command, the control algorithm will begin to actuate in the opposite direction of the aerodynamic moment. Hence, a long tail is obtained.

By analyzing the closed loop pole/zero pattern the same conclusions can be obtained. In Figure 5, the poles related to the transient behavior are slightly different from the specified. This was already expected, because the dipole is neglected during the pole placement. The important feature of this pole-zero map is the position of the pole and zero related to the coupling between the rotational and the translational movement. Note that, in the PD case, the pole related to the translational movement is on the left side of the zero. Then, the system will converge to the steady state to the top of the command. On other hand, in the PID case, the closest pole to the origin is on the right side of the zero, so that the system will converge to the steady state condition to bottom of the command profile. In both cases, the settling time is given by the closest pole to the origin.

Figure 5-Pole and zero pattern of the closed loop transfer function

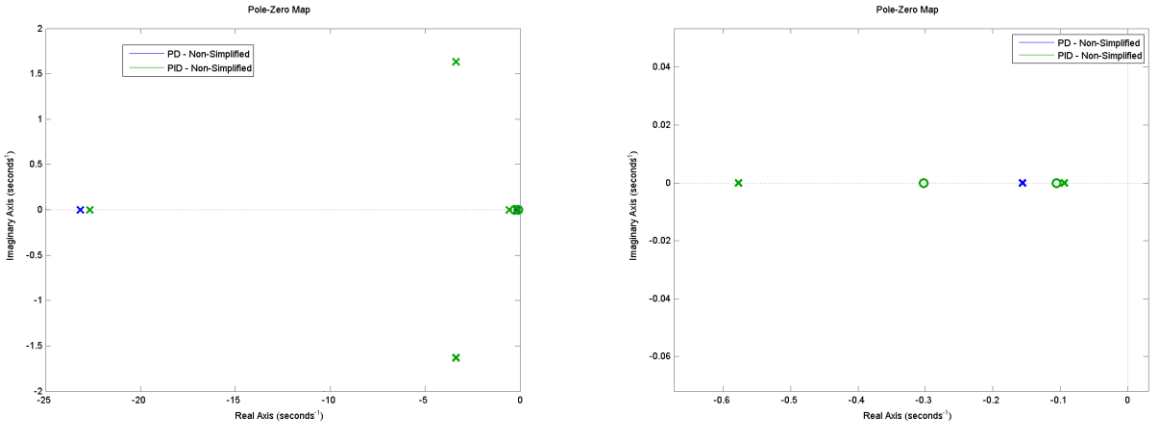

By returning to the analysis of the PD and PID controllers, note that both transient responses are similar, in spite of a small difference between the non-simplified and the simplified dynamics. Furthermore, both have an undesirable overshoot. In the PD case, the steady state level is quite different when the non-simplified and simplified responses are compared. It occurs because this simplification does not represent the static gain properly. In the PID case, the steady state error is null due to the system is of type I. The only difference between the non-simplified and simplified cases is that the response follows the reference by the bottom side for the first case.

In Figure 6, the Bode diagrams are shown for both controllers. During the analysis of the stability margins, some dynamics are not considered such as the bending modes, filters, sensor dynamics, and computation delay. Hence, as we can see, the PD offers a better stability margin than the PID controller.

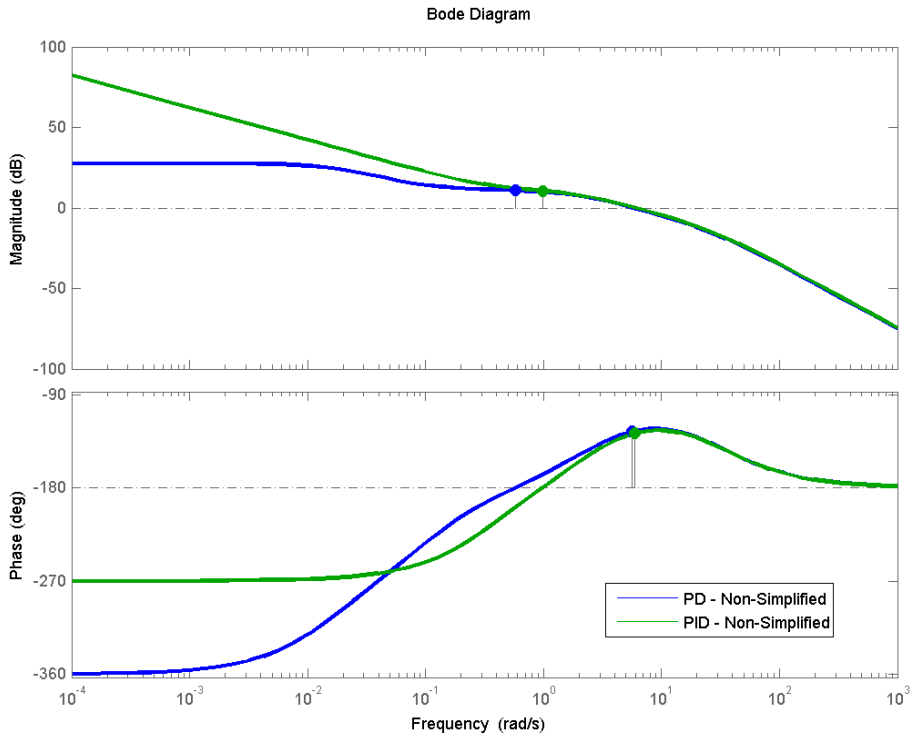

Figure 6- Open loop bode diagram of the attitude control system

Therefore, the designer should carefully analyze the results because they can lead to a wrong choice of the controller structure. For example, by considering that an optimization algorithm is applied to calculate the PD gains based on the settling time and steady condition requirements, problems can be found if the second order model is used. In this case, the algorithm would increase the proportional gain to try to reduce the steady state error. However, due to the bending mode stabilization requirement, this gain has an upper limit given by the maximum bandwidth allowed to reduce the iteration between rigid body and bending mode. If the third order transfer function is used, the PD may still be unsuitable to the problem, due to the long settling time. In this case, the choice of the PID would be still maintained. Based on this discussion, an analytical model to the rigid body and a different type of structure will be proposed to face these questions.

3. Rigid Body Alternative Model

The rotational poles properly represent the high frequency dynamics and the product of these poles is approximately μ_α. Then, by applying the polynomial property, whose the independent term is equal to the product of all roots [6], it is possible to write the independent term of Eq. (1) as

$$p_3\mu_\alpha = \frac{g\mu_\alpha \cos\theta_0}{u} \tag{11}$$

where p_3 is the third pole of Eq. (1). Then, the rigid body equation is written as

$$G_p(s) \approx \frac{\mu_\beta}{\left(s^2 - \mu_\alpha\right)} \frac{\left(s + Z_\alpha/u + Z_\beta\mu_\alpha/\mu_\beta u\right)}{\left(s - g\cos\theta_0/u\right)} = G_s(s)L(s) \tag{12}$$

where L(s) is the additional term to represent the rigid body dynamics.

Note that, the pole related to the translational motion is always unstable. These equations properly represent the rigid body dynamics, as it can be seen in Figure 7. The additional term introduced into the rigid body dynamics are similar to a lead/lag structure, which the pole is located approximately at the origin.

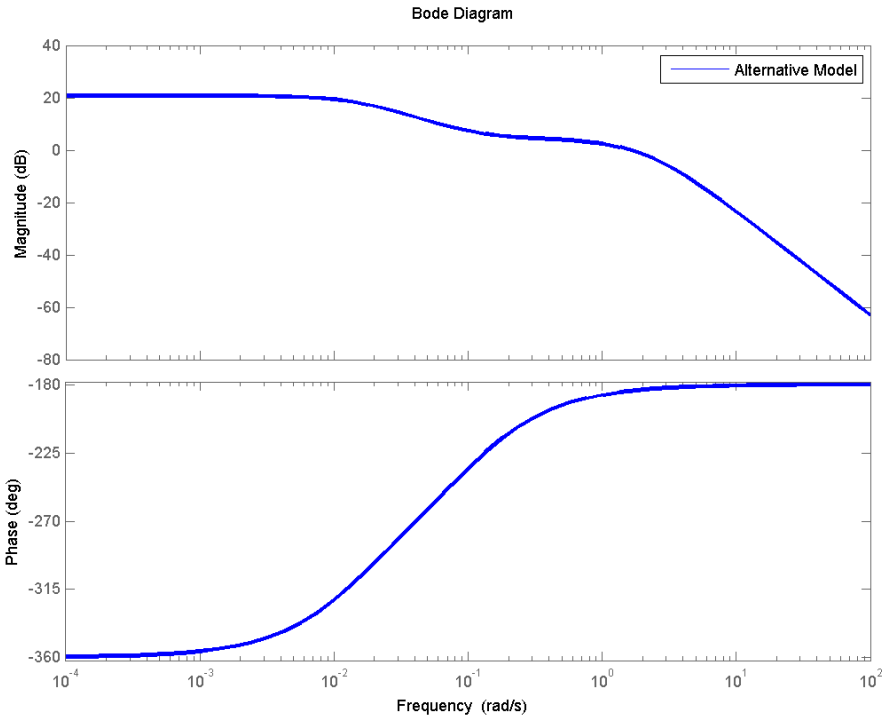

Figure 7-Alternative model rigid body dynamics

The static gain of the Eq. (12) is

$$G_p(0) = -\frac{\mu_\beta}{\mu_\alpha}\frac{Z_\alpha}{g\cos\theta_0}\left(1 + \frac{l_\alpha}{l_c}\right) = G_s(0)L_1(0)\,. \tag{13}$$

Note that, if Z_α is higher than $g\cos\Theta_0$, the static gain will be also higher for the non-simplified model. This situation happens to strongly unstable rockets. Therefore, the steady state error decreases in a stable closed loop, but, as we saw in the previous section, the settling time cannot be satisfactory in some cases.

When the rocket is strongly unstable, it is advisable to use Eq. (12) to design the controller, so that some vehicle features are not lost. In the next section, a different type of control structure will be presented.

4. PD plus lag structure

In section 1.3, it was shown that the PD has a better overshoot and stability performance than the PID case. However, the settling time is not satisfactory. The settling time is given by the translational pole, which is attracted by the zero. For the PD case presented in Figure 8, however, if a phase lag is inserted in series with the plant dynamics, the steady state error, settling time and overshoot decrease. The Eq. (14) of phase lag is given by

$$P_L(s) = \frac{s + z_L}{s + p_L} \tag{14}$$

where p_L and z_L are the phase-lag pole and zero respectively.

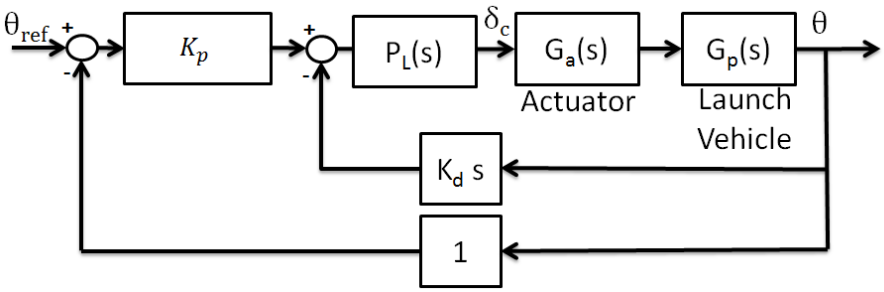

Figure 8-Phase Lag structure

The phase-lag can be designed by following the insights obtained by the pole/zero patterns. To reduce the settling time, we should increase the aerodynamic coupling frequency, which is given mainly by the zero. The plant zero cannot be changed unless the vehicle physical characteristics also change. However, the vehicle zero can be artificially canceled by placing the phase-lag pole exactly over it. In addition, the phase lag zero is placed further from the origin than the vehicle zero by aiming proper state steady error, settling time values and a minimum stability margins reduction. This new zero location will attract the translational pole.

By considering the vehicle parameters given on Table 1 and the plant dynamics given by Eq. (12), the PD gains and the phase-lag compensator are then calculated. The PD design is performed at the same way of section 1.2 to keep the required gain crossover frequency. As discussed above the phase-lag pole will cancel the plant zero. The phase-lag zero is heuristically chosen to increase the system static gain and to reduce the settling time, the overshoot and to keep proper stability margins. In this way, the PD gains are chosen as K_p = 2.20, K_d = 0.84, and the phase lag is tuned so that z_L = 0.73 and p_L= 0.1055.

The three architectures are compared in Figure 9. It is clear that the PD plus phase-lag offer better time domain response than the other structures. However, the stability margins are deteriorated. An aspect concerning this type of configuration is that the pole-zero cancellation does not occur in practice, due to the plant coefficients are not known exactly. As a consequence, there is the possibility of the hidden dynamics occurrence if the system is affected by disturbances.

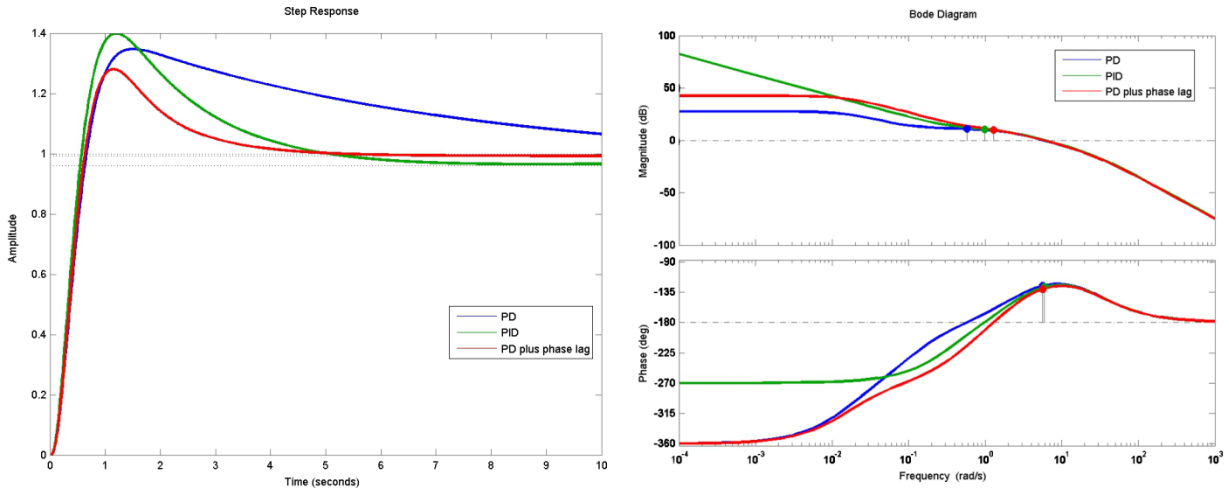

Figure 9-Step Response and Bode diagram of the attitude control system

5. PD plus phase-lag controller robustness

The attitude control system robustness is an important feature since the parametric uncertainties. A good robustness indicative is given by the stability margins [1]. Such robustness is verified through a complete simulation, which includes the bending modes, filters, sensor dynamics and a more detailed actuator model. Moreover the maximum actuator deflection is limited to 3° in the time domain simulation.

In Figure 10, the step response is shown for the three architectures. Note that all the systems show an oscillation. This occurs due to the low stability margin of the rigid body related to the high level of the control bandwidth. This bandwidth was necessary to reduce the steady state error (section 2).

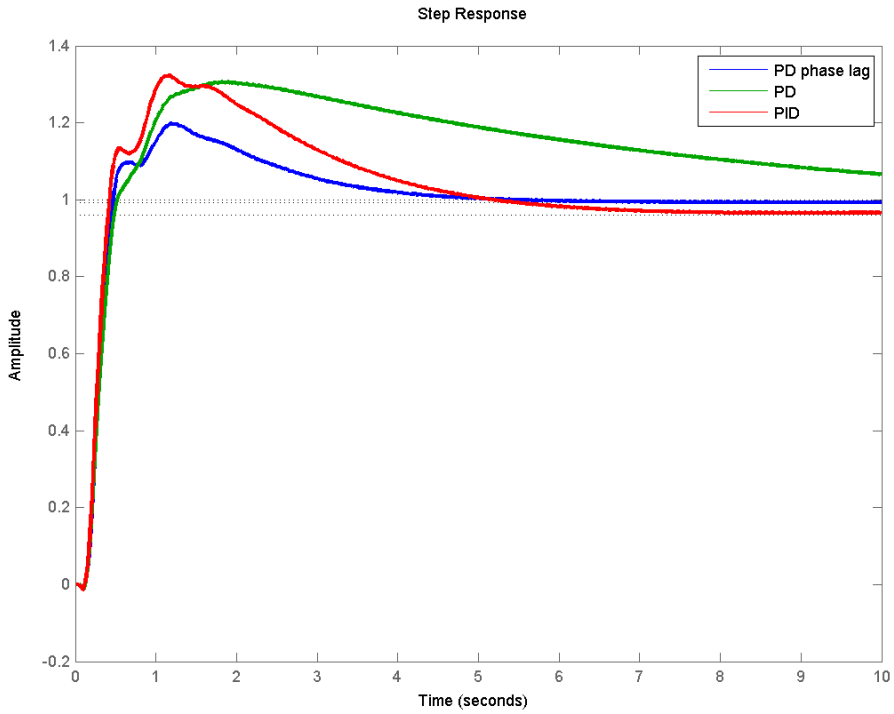

Figure 10-Step response of the complete model

Thus, the rigid body bandwidth should be reduced to improve stability margins. This is performed by decreasing the complex poles natural frequency of the rigid body. In Figure 11, the step response and Nichols chart are shown. As it can be seen, the step response is very smooth and the stability margins are satisfactory.

Two other simulations are performed to test the attitude control system robustness for non-nominal cases. In the first one, the vehicle pilotability is reduced, by decreasing μ_β and increasing μ_α by 10%. On other hand, the second case considers an increasing of pilotability, by switching the relations above. In Figure 12 the step response of the both cases are shown.

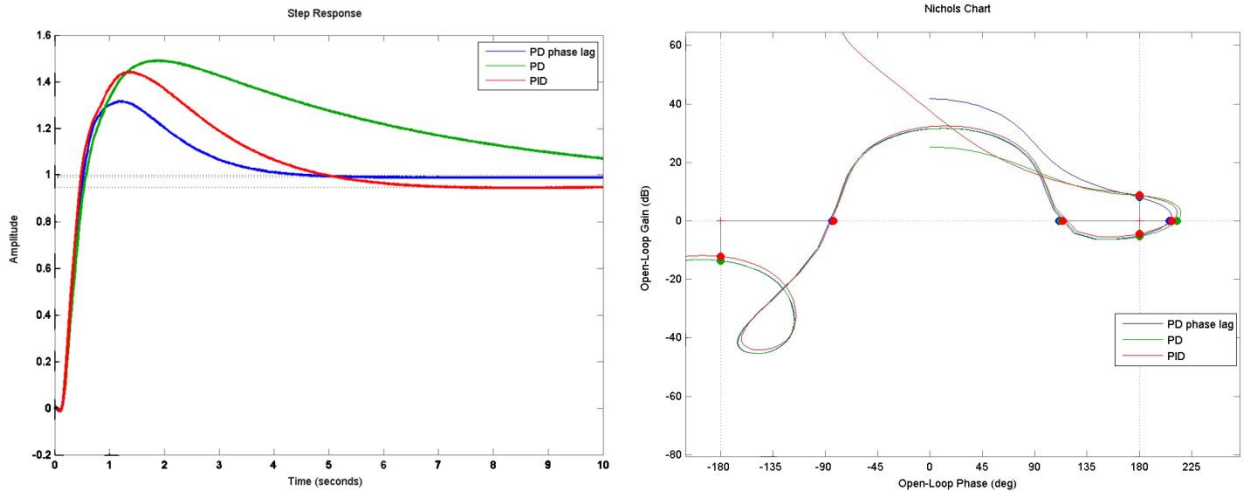

Figure 11-Step response and Nichols diagram

Even though the system pilotability is reduced, the PD plus phase-lag still achieves the requirements, in spite of the overshoot increases by small quantity. On other hand, if the system pilotability is increased, the step responses are similar to the nominal case.

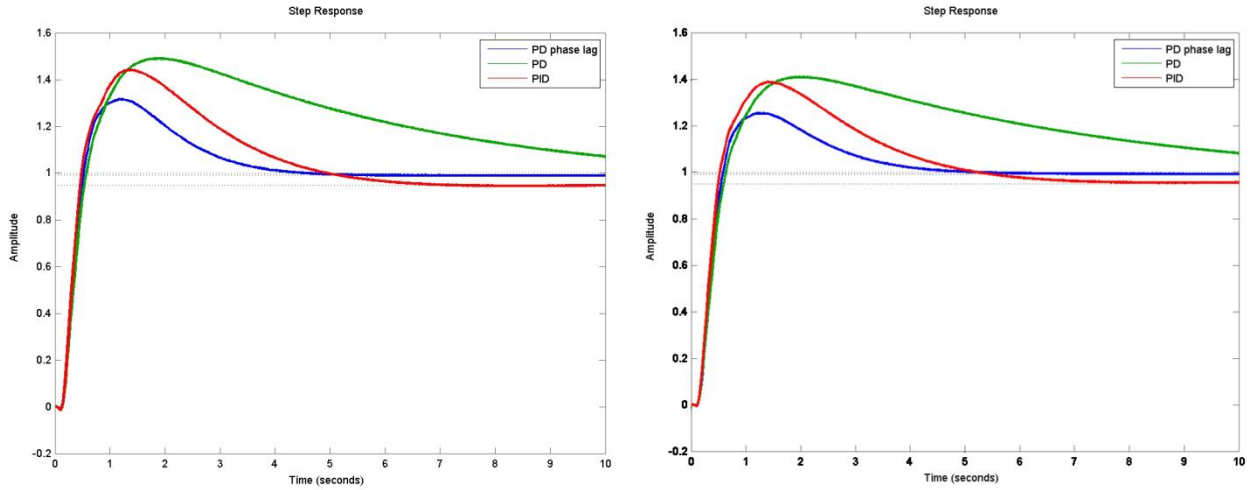

Figure 12- Non-nominal step responses cases respectively

6. Conclusions

This paper pointed out that the rigid body simplified transfer function is not suitable to evaluate the time domain requirements and the complete transfer function should be used when a highly unstable vehicle is considered. Moreover, it was shown that the pole/zero pattern can offer good insights about the vehicle dynamics. At the regions of high dynamic pressure, PD and PID controllers cannot be suitable to achieve the time domain requirements. Then a PD plus phase-lag architecture was proposed to overcome this problem. This architecture gives a better time

domain response and keeps the stability margins at acceptable levels. More studies should be carried out to evaluate the architecture behavior during the whole atmospheric flight. Furthermore, if the load relief is the main requirement to the attitude control system during the high dynamic pressure region, the PD plus phase-lag architecture may not be also suitable.

Acknowledgment

This work has been supported by SIA-FINEP/FUNDEP project.

References

[1] Whorton, M., C. Hall, and S. Cook. 2007. Ascent flight control and structural interaction for the ares-I crew launch vehicle. *Proceedings of the 48th AIAA/ASME/ASCE/AHS/ASC on Structures, structural dynamics and materials conference*, Honolulu, Hawaii

[2] Greensite, L. A. 1970. Analysis and Design of Space Vehicle Flight Control Systems, New York, US: Spartan Books.

[3] Kadam, N.V. 2009. Practical Design of Flight Control Systems for Launch Vehicles and Missiles. Allied Publiser. New Delhi

[4] Renault, C. Sanouis, 2008. P. Launchers Control Architecture and Synthesis with Analytical Loop. European Conference for Aerospace Sciences (EUCASS)

[5] Jang, J .W, Alaniz. A, Hall, R. Bedrossian, N. 2010. Ares I Flight Control System Design. *AIAA Guidance, Navigation, and Control Conference*, Toronto, Ontario Canada

[6] Wylie, C.R. 1975. Advanced Engineering Mathematics, McGraw-Hill, Tokyo, pp. 533.